CHAPTER 4:

Multilevel Modulation in *C.elegans* Sleep

Submitted for publication as Julie Cho & Paul Sternberg. “Multilevel Modulation of a Sensory Motor Circuit in *C. elegans* Sleep”

4.1 ABSTRACT

Sleep is essential for human and animal health and is behaviorally characterized by its circadian timing, behavioral quiescence, homeostasis, increased arousal threshold, and rapid reversibility. Behavioral evidence suggests that our perception is dramatically dampened during sleep, and that there are physiological changes within individual neurons and their connections to each other. However, there are many ways to dampen arousal, and despite studies spanning mammalian and non-mammalian species, the circuit modifications that promote sleep behavior are largely unknown. Here we systematically dissect components of a sensory motor circuit and identify changes in the flow of information from sensory to inter- and motor-neuron that implement sleep-like behavior in the nematode *Caenorhabditis elegans*. We demonstrate that the top two layers of sensory processing are affected, with decreases in both sensory transduction and subsequent transmission of this information to interneurons. Modulation in transmission results in a decreased likelihood of coordinated activity in the downstream interneurons, which can be reversed with sufficient prior sensory stimulation. Multilevel depression provides an elegant strategy to promote a robust decrease in arousal while allowing for rapid reversibility of the sleep state.

4.2 INTRODUCTION

Sleep behavior is conserved and present in essentially all animal species as a lack of reactivity to sensory inputs, low activity, decreased conscious awareness, and rapid reversibility to wakefulness.[1,2] Despite long-standing knowledge and characterization of these states, translation to a physiological or circuit definition has been difficult for many reasons. No single molecular or neuronal pathway has been shown to be responsible for the regulation of sleep, and incomplete knowledge of connections in sensory motor circuits of many studied species precludes interrogation of the flow of information that promotes sensory responses. Furthermore, the complexity and redundancy of the mammalian nervous system complicates the understanding of the flow of information. Here we use the nematode *C. elegans* to define sleep behavior in a simple sensory motor circuit.

C. elegans exhibits sleep-like behaviors during lethargus, a quiescent state during which locomotion and feeding are suppressed[3] and sensory arousal is decreased[4]. Lethargus lasts two to three hours, and like sleep it exhibits homeostasis: upon disruption or deprivation during the

normal resting period, there is a period of anachronistic rebound rest.[4] During lethargus, worms exhibit delayed or decreased avoidance behavior in response to both mechanical and chemical stimuli, and this response delay is reversible upon previous stimulation of the same neuron.[4] It is of note that quiescence as measured by decreased feeding and locomotory behavior is present in adult satiety behavior.[5] However, the dynamics of this state were not previously studied.

Lethargus invariably occurs during development after each of the four larval stages, and the timing of lethargus corresponds to increased expression of LIN-42, homolog of circadian regulator PER.[6] In addition, several additional conserved regulators have been identified. Anachronistic quiescence is also induced by expression of EGF[3], a function conserved in mammals[7] and Drosophila[8], and sensory arousal can be depressed by PKG[4], another well-conserved signaling protein. Conservation of sleep characteristics and molecular signaling suggests that the lethargus state in *C. elegans* could prove insightful in understanding sleep regulation.

The connections of the *C. elegans* nervous system are mapped[9,10], and functional circuits mediating avoidance defined[11]. Avoidance behaviors are mediated by mechanosensory and chemosensory neurons that activate downstream circuit components to coordinate motor neuron activity and locomotion. The ASH sensory neuron drives an avoidance circuit and promotes immediate locomotory reversal. When animals are presented with ASH-specific stimuli, ASH stimulates interneurons AVA and AVD, which in turn induces backward locomotion through stimulation of excitatory cholinergic motor neurons in the ventral cord (Figure 1a).[12,13,14] Evidence of changing arousal as measured by response delay to ASH-specific stimuli suggests modulation in the avoidance circuit during sleep behavior.

Many tools exist to probe and study neural circuits in *C. elegans*. Use of known transcriptional control regions of characterized genes drive expression of genetically encoded calcium sensors and allow measurement of activity in single or multiple cells. Cameleon is a dual channel ratiometric reporter that corrects for changes in reporter expression over states, stages and time. However, Cameleon has slower dynamics because it involves energy exchange between two fluorphores, and GCaMP, a single channel reporter, has better dynamic range. Therefore, we used both reporters: cameleon controlled for state-related changes in reporter expression and GCaMP allowed measurement of smaller calcium events. Activity patterns observed can be mimicked using light-driven cation channels such as channelrhodopsin (ChR2). Similar to the calcium sensors, ChR2 is genetically encoded and expression in select cells using specific promoters as well as combinatorial approaches that allow expression only where two promoters overlap[15] or that allow expression only in cells that are unique to one promoter in the pair[16]. These strategies allow

measurement and activation of specific components of pertinent circuits. Here we use genetically encoded calcium sensors and light-driven channels to investigate the ASH circuit during sleep and waking. We find that multiple steps in the circuit are dampened during sleep.

4.3 ASH SENSORY NEURON EXHIBITS DECREASED SENSORY RESPONSE

The amphid sensory neuron, ASH, senses multiple aversive stimuli, including mechanical stimulation at the tip of the head, and noxious chemical cues, such as copper, 1-octanol, or high osmolarity.[13] We used a chemical stimulus to characterize ASH activity during a "sleep cycle" because it is more consistent and controllable than mechanical stimuli. We fabricated a modified version of a microfluidic olfactory chip[17] to accommodate and immobilize fourth larval stage (L4), lethargus, and young adult animals (Figure 1B). These devices permitted temporally controlled delivery of chemical stimuli and simultaneous fluorescence imaging from the ASH. Individual animals were assayed for a six-hour period, during which they were subjected to a brief stimulus every 30 minutes. ASH response was measured during these intervals using the calcium indicator GCaMP3.[18] Each animal was imaged before, during and after lethargus. Chemosensory neurons use ligand-binding receptors to open ion channels[11], and ASH responds to the addition of 1mM Cu^{2+} with a robust influx of calcium in the L4 stage. During lethargus, the magnitude of ASH response decreases significantly to copper or glycerol, but full responsivity is recovered upon exit from lethargus (Figure 1C, S1A).

To confirm this result and control for confounding factors such as changes in GCaMP expression and baseline calcium levels, short assays were performed using ratiometric imaging with the calcium sensor Cameleon.[18] In these assays, animals of each stage were loaded into the device, imaged within an hour of loading for both baseline and stimulus measurements, and discarded. These short assays were consistent with the longitudinal analysis: there was significant decrease in calcium influx as measured by the peak fluorescence change in response to the chemical copper and glycerol (Figure 1D-E, S1A). Moreover, the availability of fluorescent indicator and baseline calcium concentration did not change sufficiently among behavioral states to account for the decrease in influx (Figure S1B-C). Therefore, the calcium imaging data indicate that there are fewer calcium channels open, and thus the same stimulus is less able to excite the ASH sensory neuron during lethargus. This result is consistent with decreased calcium dynamics observed in the mechanosensory neuron, ALM, during lethargus.[19] Furthermore, stimulus-evoked calcium transients were not ligand specific as evidenced by decreased response to both copper and

glycerol and suggest that modulation in lethargus may affect general excitability or synaptic activity of the ASH neuron.

4.4 BASAL ACTIVITY OF AVA IS SUPPRESSED IN LETHARGUS

GCaMP3 findings were confirmed with Cameleon measurements at the interneuron level. Calcium levels in AVA oscillate and increasing levels correspond with reversals.[20] We observed that oscillation of AVA activity is not regular and disappears in lethargus, but reappears in the young adult animals (Figure S3A-B). Therefore, the basal activity and the context in which AVA receives input from ASH changes during lethargus.

4.5 SYNCHRONY BETWEEN AVD AND AVA IS LOST IN LETHARGUS

To assess activity across the top two layers of the circuit, we used animals expressing GCaMP3 in ASH, AVD, and AVA. To examine stimulus-driven interneuron activity, we measured responses to ASH-specific cue (1M glycerol)[12], which has less variable dynamics (Figure S1A). Each 60-second trial consisted of a 10-second pulse of control buffer or glycerol. Trials with discernable ASH responses were chosen, and instantaneous slopes were calculated over the imaging interval to represent the magnitude of the calcium influxes. In young adult animals without stimulation, the timing of the calcium influxes showed no association with the pulse of the control buffer and did not occur during the stimulus interval (Figure S2B). However, after a glycerol stimulus, the influx of calcium in the AVD and AVA was associated with the stimulation interval (Figure 2B-C). AVD and AVA showed both decreased responsivity during lethargus as well as a loss of coordinated calcium activity. Animals in lethargus exhibited very little activity in the AVD and AVA, and fluctuating calcium levels during the glycerol stimulus were not significantly different from the period preceding the stimulus (Figure 2B). Because the magnitude of activity is considerably smaller in lethargus compared to the young adult, we had to normalize these measurements as binary values. Positive changes in fluorescence were thus counted as individual influx events. There were significantly more influxes during the glycerol stimulus in the young adult, but often little activity was seen in AVA during lethargus even when AVD activity was noted (Figure 2C-E).

To test for association of ASH-interneuron and AVD-AVA activity, we compared the timing of initiation and duration of the calcium transients between neuron pairs by performing cross

correlation analysis between each of the neurons imaged. Comparing data for timing between of calcium events between pairs allows us to assess functional correlation between neurons. This cross correlation analysis indicates that when compared to the input ASH neuron, AVD transients exhibit a lag during lethargus, whereas AVA transients do not (Figure 2D-E). This observation suggests that when awake AVD and AVA receive a signal from the ASH and exhibit simultaneous calcium transients, whereas AVD in a lethargus animal is desynchronized with AVA. We further analyzed AVD and AVA for instances of repetitive calcium transients. There was a significant decrease of coupled trains during lethargus; a majority of the traces did not show activity in both neurons, and uncoupled activity was present during lethargus (Figure 2F-G). Moreover, the number of AVA only traces did not differ significantly from the number of AVD only traces (Figure 2G), suggesting that alterations of synaptic transmission are not specific to a particular synapse.

These results indicate that coupled activity in the command interneurons occur in the awake state and may not only explain processing delay during lethargus but also suggests that synaptic transmission downstream of ASH becomes variable and differs across independent synapses. The altered efficacy of ASH-AVD and ASH-AVA synapses could be due to decreases in either presynaptic transmission or postsynaptic excitability. However, while it is possible that the ASH compartment presynaptic to AVD may vary independently from that which is presynaptic to AVA, the calcium measurements in the ASH show no indications that this is the case. In addition, synapse specific changes or lags in activity usually show a general preference for a specific synapse rather than random or equal distribution as indicated by our AVD and AVA measurements (Figure 2G). The simplest interpretation of the result is that there are postsynaptic changes in the downstream neurons.

4.6 LOSS OF SYNCHRONY IS REVERSIBLE

Delayed response could also be a way for the circuit to function in all states (both awake and lethargus) when calcium activity in the ASH in decreased. In fact, decreased avoidance response to ASH-specific stimuli has been attributed to decreasing calcium activity in dopamine-treated animals.[15] Although neuromodulator-mediated sensory dampening is seen as decreases in behavioral response in the presence of serotonin or dopamine[15], reversibility in behavior is more specific to the sleep state. Furthermore, the source of reversibility is unknown, and it is important

to identify whether reversibility is reflects as reversibility in magnitude of calcium influx or in the response of downstream components.

Therefore, we measured lethargus animals expressing GCaMP in ASH, AVD, and AVA in the microfluidic chip with and without a mechanical stimuli preceding glycerol stimulation. Individual animals showed the same trend: calcium influx in the ASH did not differ significantly between unperturbed and perturbed trials (Figure 3A-B), but the activity in the downstream interneurons was both coordinated and immediate in trials following mechanical stimulation (Figure 3A). This result indicates that although varying presynaptic input from the ASH may change circuit function and behavior, there are other postsynaptic factors that modulate transmission at these synapses. Furthermore, these changes are dependent upon previous stimulation at the level of the interneurons.

4.7 MODULATION ALSO LIES DOWNSTREAM OF ASH DEPOLARIZATION

We validated imaging data and assessed the contribution of downstream neurons to lethargus behavior using the genetically encoded light-activated cation channel Channelrhodopsin2 (ChR2). In the presence of its cofactor, all-trans retinal (ATR), ChR2 allows control of both the extent and timing of cellular depolarization through optical stimulation.[21,22,23] Changes in the sensory response to ASH-mediated noxious stimuli (such as copper or glycerol) is modulated by the presence food or exogenous application of dopamine, but these responses are modality-specific and are absent in response to mechanical stimuli.[15] Optogenetic activation of ASH was shown to be unaffected by changing conditions.[15] Direct control of ion channels and normalization of the initial current injection allows for better assessment of the downstream components of the avoidance circuit by bypassing ligand-binding and associated membrane depolarization in ASH.

Neurons classes in each level of the avoidance circuit were individually depolarized. We used animals in which ChR2 is expressed exclusively in the ASH by the use of FLP recombinase[15], and found that light-driven activation induced robust and active reversal behavior in both the L4 and young adult animals (Figure 4B). However, behavioral response delay persists upon ChR2-mediated ASH depolarization during lethargus: the average time to respond to the ChR2 stimulation increased from 2 seconds to 18 seconds in lethargus (Figure 4B). Therefore, behavioral delay is not likely due to the decrease in receptor associated depolarization at the ASH, is different from dopamine-mediated modulation, and suggests the existence of additional modulation in downstream components of the circuit.

4.8 ACTIVATION OF MULTIPLE COMMAND INTERNEURONS PROMOTES AWAKE-LIKE BEHAVIOR

We next activated the downstream command interneurons using the *nmr-1* transcriptional control region to drive ChR2 in AVA, AVD, and AVE (Figure S7A). AVA activity promotes avoidance behavior[24], and upon direct depolarization of the reverse command interneurons, animals both in and out of lethargus responded immediately (Figure 4C). We further tested animals expressing ChR2 in AVA and RIM. RIM is an interneuron associated with reversal: osmotic shock using glycerol induces a calcium influx into RIM[25] and direct depolarization of RIM with ChR2 results in robust reversal as well as calcium influx into the AVA command interneuron[14]. However, although depolarization of AVA and RIM in an awake animal induces robust reversal[26], it fails to do so consistently or quickly in lethargus (Figure 4D-E). Moreover, lethargus animals either responded similarly to awake animals or did not respond at all (Figure 4E). Thus, if and when interneurons are activated together, a rapid behavioral response followed. The lack of a rapid response upon direct ASH depolarization indicates that transmission of excitatory information from the sensory to the interneurons is decreased or delayed in lethargus.

We cannot exclude the possibility that the inability of AVA and RIM activation to generate immediate reversal during lethargus may also indicate an altered function of RIM in lethargus. RIM has been shown to exhibit either calcium influx or efflux during initiation of reverse locomotion[25], and can elicit reversals upon activation by ChR2[14] as well as inhibition by halorhodopsin[25]. It has been surmised that activity in RIM can both inhibit locomotion directly by inhibiting the muscle while activating locomotion by activating AVA. If AVA is less responsive to RIM activation during lethargus or RIM has enhanced inhibitory or decreased excitatory function, then we would expect ChR2 to be less efficient in generating reversals. Furthermore, decreasing ChR2 expression in AVA or increasing ChR2 expression in functionally modified RIM would further suppress avoidance behavior. Therefore, we measured the expression level of ChR2 in the AVA and RIM neurons and found that it did not change significantly in and out of lethargus (Figure S7B-C). Lack of altered expression suggests that either RIM function is modified or that AVA alone is not sufficient to trigger robust reversals. In either case, multiple interneuron input is a crucial component for consistent generation of immediate reversals.

Direct activation of the cholinergic motor neurons including the VA reverse motor neurons showed no significant response latency between the response of L4, lethargus, and young

adulthood (Figure 4F), suggesting that the modulation of signaling during lethargus did not occur downstream of the AVA interneuron and remained consistent with previous data indicating that the amount of contraction did not change in lethargus.[27,28] The importance of synchronous activity in multiple neurons is a reflection of the signal amplification that occurs in the circuit to promote reversal. Amplification can occur through two not necessarily distinct mechanisms: excitation of multiple interneurons by ASH and further amplification of that signal by multiple feed forward loops in the circuit (Figure 4A).

4.9 INCREASING THE EXTENT OF ASH DEPOLARIZATION CAN ELICIT IMMEDIATE RESPONSE

Previously published work describes the avoidance circuit as a coherent type 1 feed forward loop, the dynamics of which have been modeled (Figure S4A).[29] This circuit motif creates delay by preventing processing in the AVA until both ASH and AVD are active.[29] Our simulation of dynamics using the published model shows that adjusting the threshold or ratio of transfer at the ASH to interneuron synapses (even in the absence of input change) can cause a delay, which can be shortened by increasing activity at the ASH (Figures S4B; S5B). We therefore stimulated ChR2-expressing ASH neurons in a graded manner. To more strongly activate ASH, we used a 100-fold higher concentration of ATR and a 2.5-fold stronger light intensity. When subjected to this stronger stimulus, animals in lethargus displayed a reduced behavioral delay not significantly different from that of young adults (Figures 5C; S6A-B). These results are consistent with the model and suggest either the threshold or transfer at the synapse changes during lethargus, requiring significantly more presynaptic depolarization to elicit an immediate response. Increasing ASH input should increase activity at the AVD as well as the AVA, implying that the increased input to motor neurons may no longer be linear and possibly exponential. Increased current injection at RIM and AVA does not suppress response delay (Figure 5E), raising the possibility that a single command interneuron may not be able to output sufficient signal to the motor neurons to generate immediate response and that synchronous activation of the command interneurons is likely necessary for rapid reversal.

4.10 RESPONSE DELAY TO ASH DEPOLARIZATION IS REVERSIBLE

To further understand the decreased transmission between sensory and inter-neurons during lethargus, we stimulated interneurons through an ASH-independent circuit (Figure 5A). Mechanosensation at the body wall promotes reversal by activating the AVA and AVD command interneurons independent of ASH.[30,31] FLP, a mechanosensory neuron, responds to harsh touch to the anterior body.[30,32] When animals are woken by a harsh touch, they reverse immediately. After a full reversal, animals are more responsive to ChR2 stimulation, and the average response delay to ChR2-induced ASH depolarization is 2s, suppressing the response delay normally seen in lethargus (Figure 5B). Surprisingly, promoting forward locomotion using PLM/PVM-mediated tail touch, which functionally should inhibit AVD and AVA, also suppressed response delay (Figure 5B). It is thus not important whether the animals are moving forward or backward, but that they are active. Waking the animal during lethargus does not suppress response delay to AVA depolarization (Figure 5D), indicating that input into multiple command neurons is required. These results suggest that there is an awake state that determines the interneuron resistance to signal processing, and waking primes the interneurons to respond to sensory stimuli.

4.11 CIRCUIT MODULATIONS IN LETHARGUS ARE GENERAL AND DEPENDENT ON AROUSAL STATE

Behavioral quiescence can be observed outside of lethargus and in the adult stage during satiety behavior[5] and during EGF-overexpression[3]. Satiety can be induced with high nutrient food and is enhanced when a long period of starvation is followed with food[5]. We examined the behavior of animals three hours after refeeding and observed quiescence, as measured by pharyngeal pumping and locomotion (Figure 6A-B). Animals that were fasted and refed showed delayed response to ASH activation with ChR2 when compared with starved or continuously fed animals (Figure 6C). Moreover, this delay was reversible and was suppressed by previous mechanical stimulation (Figure 6D). These results show that sleep-like behavior is not restricted to lethargus and suggest the changes in the avoidance circuit is not tied to the developmental stage but physiological state of the animal.

EGF overexpression in young adult animals showed similar results. EGF signalling was implicated as a quiescence promoting component during lethargus, and anachronistic expression strongly induces quiescence.[3] Therefore, we induced quiescence by overexpressing EGF in young

adult animals (Figure 6E) and found that animals had a delayed response to ASH activation comparable to lethargus (Figure 6F). Also, delayed response due to EGF could also be reversed upon previous stimulation by a tail tap (Figure 6G). These results show that sleep-like behavior induced outside of lethargus by satiety and one component of lethargus signalling is effective in replicating the behavioral dynamics. These observations eliminate the possibility of developmental factors being the primary driver of neuronal modulation.

We also tested whether the observed sensory neuron modulation is restricted to ASH or to circuits mediating avoidance. We chose to study the gustastatory neuron, ASE, during and out of lethargus. Unlike ASH, ASE senses attractive stimuli, like preferred salt concentration, has no mechanical component, and promotes forward locomotion. We found that ASE also shows decreased calcium transients during lethargus, implying that circuit modulations are likely general across the sensory layer and similar modulation likely exist in the forward command interneurons.

4.12 DISCUSSION

We examined the well-characterized ASH avoidance circuit during sleep and waking and found that decreased arousal during sleep stems from not only the worm's inability to robustly sense the incoming stimulus but also a failure to activate components of the circuit that promote avoidance in the awake state. We found significant modulation in both sensory and command interneuron activity during lethargus and confirmed the function of observed activity patterns using channelrhopdopsin to optically control activity in single or select groups of neurons. We also find that dampened sensory activity in the ASH neuron is likely correlated with the presence of sleep drivers, is constant during lethargus, and is minimally altered in response to chemical stimuli after mechanical stimulation preceeding the measured trial duration. This neuronal activity is in stark constrast to the dynamics of behavior: sensory response to ASH activation by chemical stimuli is immediate upon previous waking with mechanical stimuli. However, changes in dynamics are well correlated with coordinated activity of the command interneurons AVD and AVA. Moreover, this coordinated activity that is lost during quiescence is recovered upon waking.

How might activation of interneurons by one sensory neuron sensitize them to other sensory neurons? One mechanism of decreasing thee threshold is to make the interneuron more receptive to presynaptic input by activity-driven changes in receptor localization.[33,34] In addition, activity-driven changes in synaptic tranmission and transfer can be readily explained by disinhibition[35] or neurotransmitter availability. The fast dynamics of the reversibility during sleep make it unlikely

that neuromodulators are directly responsible for the reversibility because unbinding from targets and breakdown or sequestration of peptides would not be possible in the time scale of behavioral dynamics (milliseconds to seconds). In addition, the mediation of reversible transmission by a secondary intermediate outside of the sensory motor circuit is precluded by the lack of candidates with the proper connectivity to all sensory neurons or even the sensory neurons published or tested in this work.[10]

Both decreased sensory transduction and reversible resistance in transmission of excitatory information downstream occurs, and the presence of these modulations pose interesting questions about the utility of having multiple levels of modulation. Decreasing the magnitude of ASH response results in decreased signal processed downstream, and theoretically, in a smaller probability of reaching threshold to relay information to downstream components of the circuit (Figures S4B, S5A). This type of sensory gating would help prolong inactivity in the sensory motor circuit and promote behavioral quiescence. However, direct alteration of the response of individual sensory neurons after waking or even all sensory neurons after waking would perpetuate a long awake state because the nervous system would not be sufficiently gated, and this might continue reponding to basal sensory stimuli as well as mechanical stimuli from locomotion. Thus, if sleep and wakefulness in the worm are regulated only by gating and lack of gating, respectively, at the sensory neuron, then the dynamics in the circuit create a positive feedback loop because activity in the circuit would sensitize the sensory neuron and promote more activity in the circuit, and so on. Furthermore, constant decrease in ASH activity makes the circuit more sensitive to small changes in signal transduction or synaptic tranmission to AVA and AVD, lengthening the range of behavioral delay and decreasing the probability of downstream synchronization (Figure S4A-B). Dynamic sensitization of the command interneurons allows for increased probability of coordinated activity upon previous stimulation, but requires sensory input to multiple command neurons (Figure 7). Therefore, the use of coordinated activity in downstream components offers flexibility and fast behavioral dynamics while simultaneously ensuring that waking leads to sensitivity to all modalities as well as sensory neurons that converge upon the command neurons.

We found that behavioral delay and reversibility is not exclusively limited to lethargus: they occur with EGF expression and with quiescence induced by satiety, indicating that these circuit modulations are due to behavioral state and not developmental stage. Thus, these results are more relevant to understanding behavioral states across species. Also, sensory dampening is likely

general in sensory motor circuits, and sensory neurons associated with food and attractive stimuli are dampened in addition to those for pain and noxious stimuli.

Past circuit understanding of sleep is limited to a general understanding of loss of synchrony between cortex and thalamus due to inability of the thalamus to relay information to the cortex.[36,37] We have demonstrated similar changes of information relay from sensory to command interneurons in a simple circuit of *C. elegans*. Decrease in sensory signaling contributes to, but is not the sole factor of, changing information relay. Excitability of the downstream command interneurons is also likely altered and serves as a point for reversible function of the circuit during the sleep-like state. Thus, small changes in dynamics at multiple levels promote and prolong quiescence while allowing reversibility of behavior upon sufficient stimulus by using components of a circuit that appear redundant, but serve to amplify or suppress input signal. The *C. elegans* nervous system is condensed when compared to a mammalian nervous system. We can then conjecture that a sensory neuron in the worm may serve to perform both sensory functions and the processing that presumably occur downstream in other less compact neural circuits. Regardless, these components of multilevel modulation serve as one strategy for generating the dynamic behaviors seen in sleep.

FIGURES

Figure 1

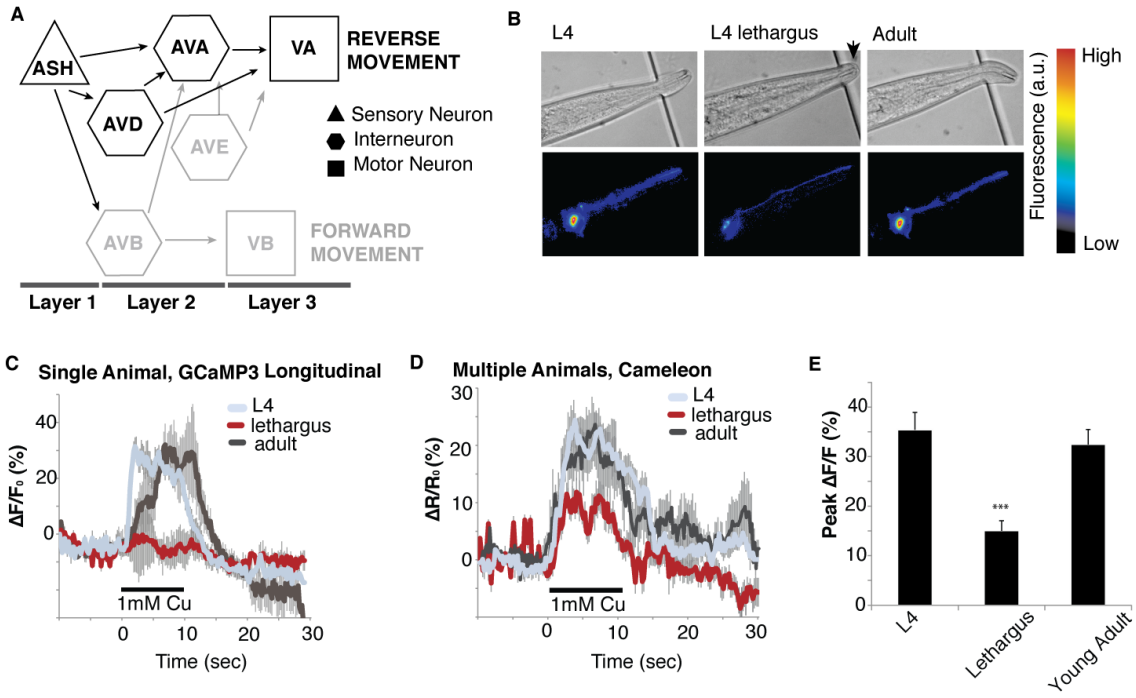

Figure 1. Sensory depression occurs in the ASH polymodal sensory neuron
(A) Functional model of the avoidance circuit. The two polymodal ASH sensory neurons work through the two AVA and two AVD interneurons to promote reversal through the VA motorneurons. Neurons tested in the study are darkened. (B) Single frames of GCaMP3 DIC and fluorescence recording in ASH over the L4, lethargus, and young adult stages. Arrow denotes the cuticle cap that marks lethargus. (C) Representative GCaMP3 traces of a single worm as it transitions from L4 to lethargus to young adult. (D) Average change in cameleon fluorescence in the ASH sensory neuron over time in a short calcium imaging assay. L4 and lethargus response to 1mM Cu^{2+} (L4 n=10; L4 lethargus n=11). (E) The calcium influx in response to 1mM Cu2+ is significantly decreased in lethargus (n=11) as compared to L4 (n=10) and young adult (n=5; ***p<0.001, Student's t-test equal variance).

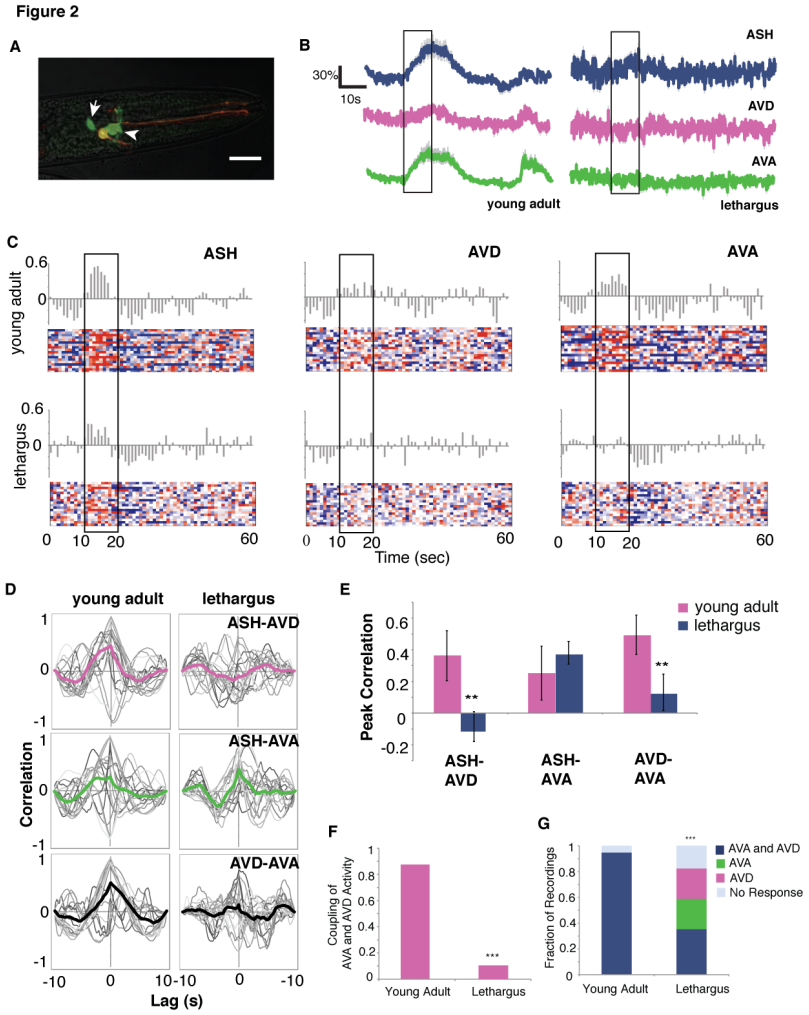

Figure 2. AVD loses synchrony with AVA in lethargus

(A) Image of the neurons in which GCaMP3 was measured. ASH is marked by the presence of both GCaMP3 and mCherry, AVD is posterior (white arrow), and AVA is anterior (white arrowhead). (B) Representative traces of a glycerol trial in a single animal in both lethargus and young adult. (C) Heat map of 60s trials denoting influx (red) and efflux (blue) in young adult (n=18) and lethargus (n=18). The proportion of influx or efflux were averaged across trials in 1s bins and are denoted by the gray bars above the heat maps. (D) Cross correlation of the stimulus interval between ASH-AVD, ASH-AVA, and AVA-AVD. Individual cross correlations are shown as gray lines, the average by the colored line. Correlation of 1 is a perfect match, and correlation of -1 denotes an inverse relationship. AVD exhibits an average lag in response and shows a decreasing correlation with AVA during lethargus. (E) Peak correlation values extracted from the cross correlation analysis. AVD loses its synchronicity with ASH and AVD only in lethargus ($p<0.01$, n=18, students t-test of unequal variance). AVA shows no decrease in correlation with ASH. (F) Quantification of trials in which GCaMP3 measurements of AVA and AVD showed corresponding trains of calcium influx during the course of the trial. The majority of trials in the young adult (0.86, n=23) showed coupled activity, but this coupling decreased significantly in lethargus ($p<0.000001$, 0.12, n=16). Many of the trials in lethargus showed activity in either AVA or AVD, while young adult animals did not show any instances of this pattern of activity ($p<0.0001$).

Figure 3

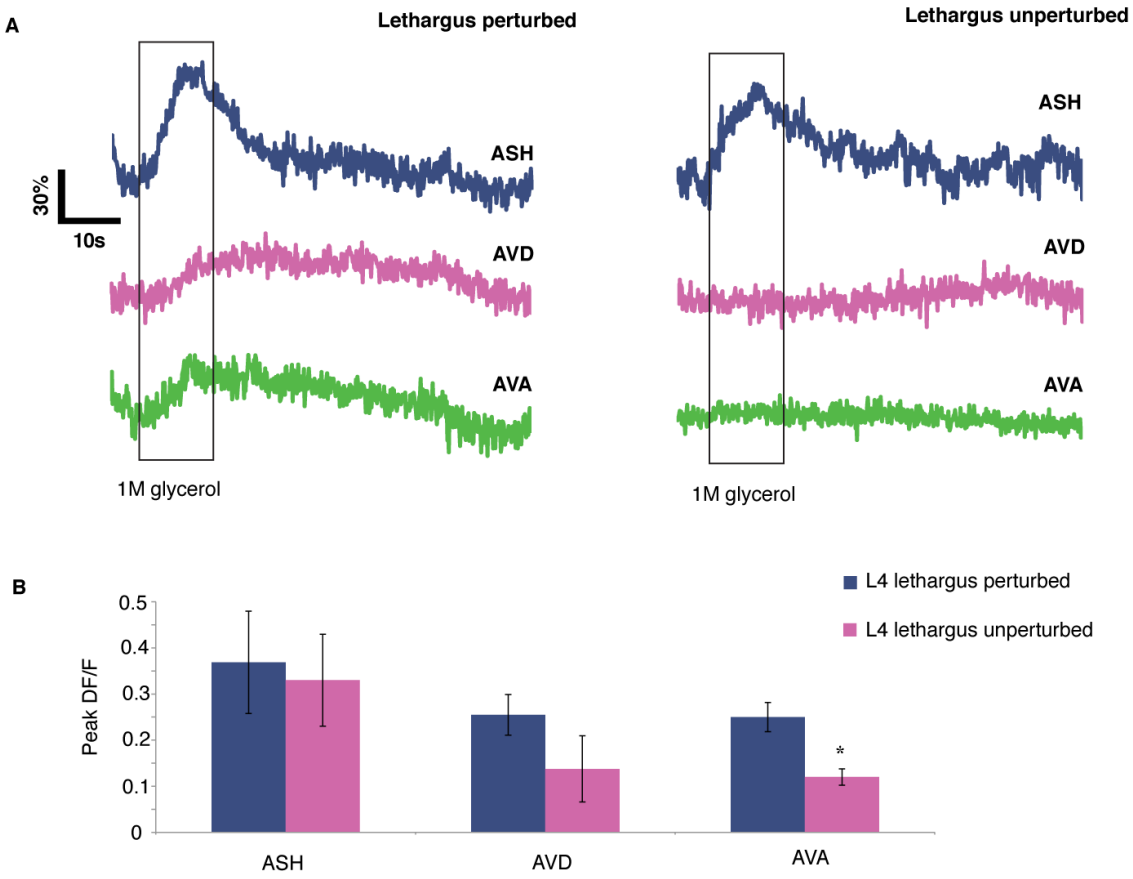

Figure 3. Loss of synchrony is reversible and can be separated from magnitude of calcium influx in the ASH

Representative GCaMP3 measurements of ASH, AVD, and AVA of a single worm in response to 1M glycerol with and without previous mechanical stimulation during lethargus. (B) Perturbation does not significantly affect peak increase in ASH as measured by GCaMP3, but it does cause significant increase in responsivity at the AVA (*$p<0.01$, $n=4$, students t-test of unequal variance).

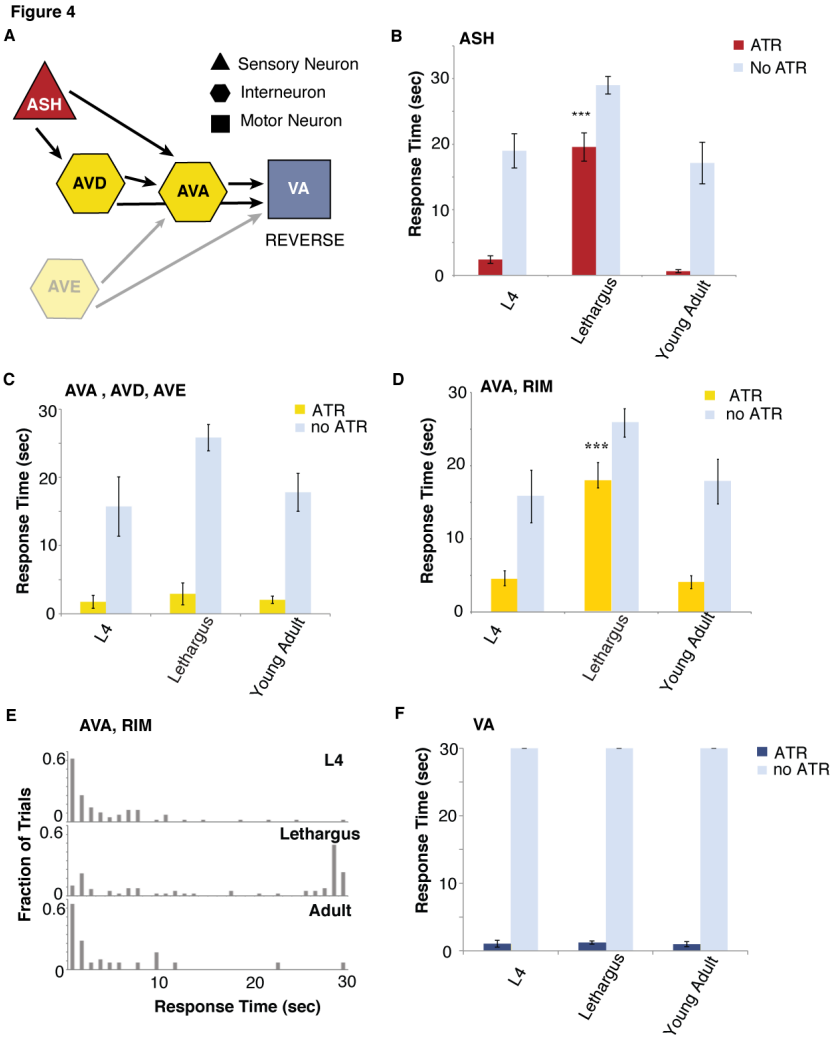

Figure 4. **Sensory modulation occurs downstream of ASH depolarization**
(A) Schematic diagram of the neurons manipulated to generate reversal. ASH promotes activity at the AVD and AVA interneurons. (B) Behavioral response times to ASH depolarization using channelrhodopsin. The mean ± s.e.m. values are shown: L4 (n=13), lethargus (n=9), adult (n=7); ***p=0.0001, ANOVA. All ATR treated animals were compared to their paired non-ATR treated controls L4 (n=13), lethargus (n=9), adult (n=7); p<0.0001, Student's t-test of unequal variance. (C) AVA, AVE, and AVD were depolarized using channelrhodopsin. Avoidance behavior did not differ significantly between worms in and out of lethargus. L4 (n=7), lethargus (n=6), adult (n=6); ANOVA. All ATR treated animals were compared to their paired non-ATR treated controls L4 (n=7), lethargus (n=6), adult (n=6); p=<0.0001, Student's t-test equal variance. (D) Depolarization of AVA without the other command interneurons showed a significant delay in lethargus (n=15) when compared with L4 (n=16) and adult (n=8); ***p<0.0001, ANOVA. All ATR treated animals were compared to their paired non-ATR treated controls L4 (n=15), lethargus (n=16), adult (n=8); p<0.0001, Student's t-test of unequal variance. (E) Distribution of individual trials show two different populations during lethargus, making reversal behavior in lethargus significantly different; ***p<0.0001, Mann-Whitney test. (F) Depolarization of cholinergic motorneurons with channelrhodopsin. L4 (n=5), lethargus (n=5), adult (n=5), ANOVA. All ATR treated animals were compared to their paired non-ATR treated controls L4 (n=13), lethargus (n=9), adult (n=7); p<0.0001, Student's t-test equal variance

Figure 5

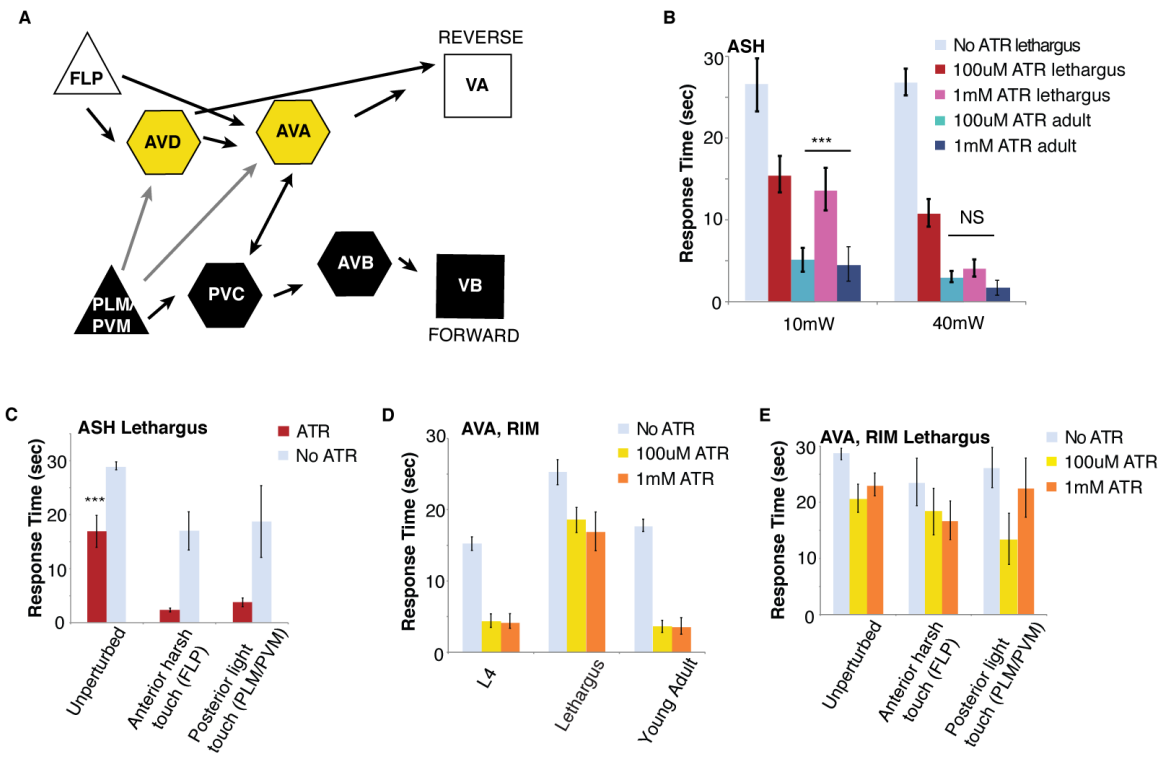

Figure 5. Reversibility arises from interneuron activation but requires simultaneous input to both AVD and AVA

(A) Schematic diagram of the neurons manipulated to generate reverse locomotion. Multiple sensory cues and neurons can induce reversal, including ASH, and FLP.[12,30] FLP neurons are activated in response to harsh mechanical stimulation at the body wall and act independently of ASH to promote activity at the AVD and AVA interneurons. The PLM and PVM mechanosensory neurons work through the PVC interneuron but are also synaptically connected with the AVA and AVD to generate forward locomotion in response to tail touch. (B) ASH of lethargus animals were depolarized with ChR2 unperturbed (n=21), after harsh touch at the body wall (n=9), and after tail touch (n=12). Both perturbations suppressed the delay in reversal; ***p<0.0001, ANOVA. All ATR treated animals were compared to their paired non-ATR treated controls unperturbed (n=21), after harsh touch at the body wall (n=9), and after tail touch (n=12); p=<0.0001, Student's t-test of unequal variance. (C) Behavioral response to 10mW and 40mW of optical stimulation of ChR2 in lethargus and young adult animals at 100µM and 1mM ATR concentrations. (D) AVA of lethargus animals grown in 0, 100µM, or 1mM ATR were depolarized with ChR2 unpertubed (n=23), after harsh touch (n=10), and after tail touch (n=13). No significant difference was seen between animals grown on 100µM and 1mM ATR. All ATR treated animals were compared to their paired non-ATR treated controls unperturbed (n=23 after harsh touch at the body wall (n=10), and after tail touch (n=13)); p=<0.0001, Student's t-test of unequal variance. (E) Even with increased ATR concentraion at 1mM, depolarization of AVA in animals continued to show a significant delay in lethargus (n=11) when compared with L4 (n=13) and adult (n=9); ***p<0.0001, ANOVA. No significant difference was seen between animals grown on 100µM and 1mM ATR.

Figure 6

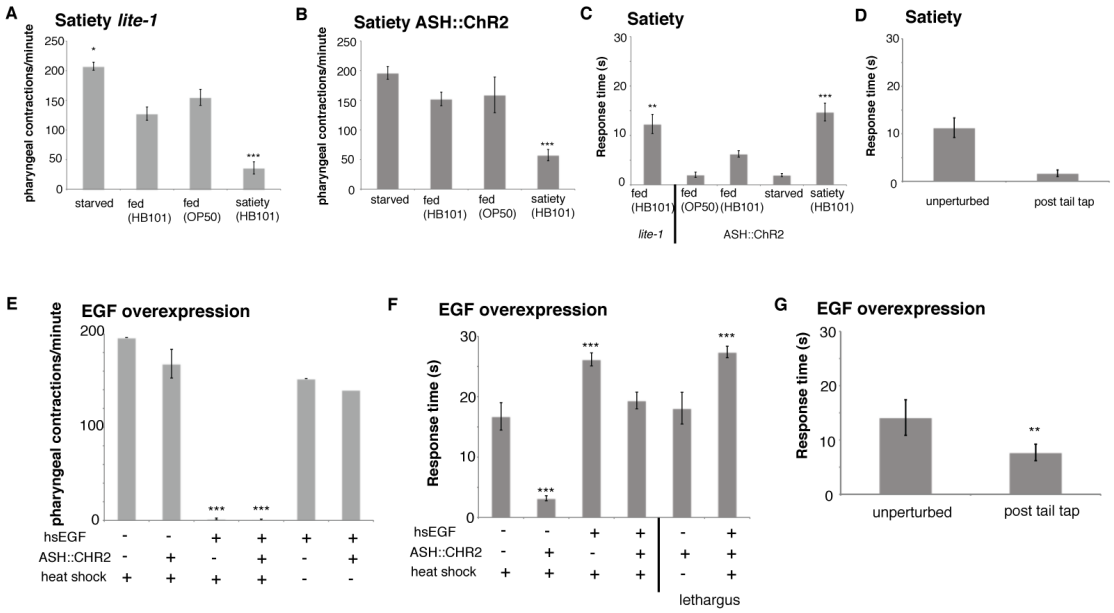

Figure 6. Circuit modulations in lethargus are dependent on arousal state

(A) Feeding activity of *lite-1* animals (which has decreased response to blue light) as indicated by pharyngeal contractions in response to starvation (n=8), feeding on OP-50 (n=9), feeding on HB101 (n=5), and feeding after 12 hours of starvation, i.e. satiety assay (n=14). The mean ± s.e.m. values are shown, *p=0.01, ***p=0.0001, ANOVA. (B) Feeding activity of ASH::ChR2 animals as indicated by pharyngeal contractions in response to starvation (n=8), feeding on OP-50 (n=5), feeding on HB101 (n=13), and feeding after 12 hours of starvation, i.e. satiety assay (n=17). The mean ± s.e.m. values are shown, ***p=0.0001, ANOVA. (C) Reversal following light activation of *lite-1* (n=8), ASH::ChR2 animals that were subjected to starvation (n=20), feeding on OP-50 (n=13), feeding on HB101 (n=8), and feeding after 12 hours of starvation, i.e. satiety assay (n=17). The mean ± s.e.m. values are shown, **p=0.001, ***p=0.0001, ANOVA. (D) Reversal following light activation of ASH::ChR2 animals following the satiety assay before perturbation (n=11) and after tail tap (n=11), ***p=0.0001, Student's t-test of unequal variance. (E) Feeding activity as indicated by pharyngeal contractions were measured to assess activity levels of the animals following EGF overexpression by heat shock. Only animals with the heat shock EGF transgene (hsEGF) that were treated with heat shock showed decrease in activity. The mean ± s.e.m. values are shown: heat shock *lite-1* (n=5), heat shock ASH::ChR2 (n=5), heat shock hsEGF (n=11), heat shock hsEGF ASH::ChR2 (n=7), hsEGF (n=5), ASH::ChR2 (n=5), ***p=0.0001, ANOVA. (F) Reversal following light activation of heat shocked animals. The mean ± s.e.m. values are shown: heat shock *lite-1* (n=11), heat shock ASH::ChR2 (n=17), heat shock hsEGF (n=18), heat shock hsEGF ASH::ChR2 (n=16), heat shock ASH::ChR2 in lethargus (n=10), heat shock hsEGF ASH::ChR2 in lethargus (n=9), ***p=0.0001, ANOVA. (G) Reversal following light activation of hsEGF ASH::ChR2 animals following before perturbation (n=11) and after tail tap (n=11), ***p=0.0001, Student's t-test of unequal variance.

Figure 7

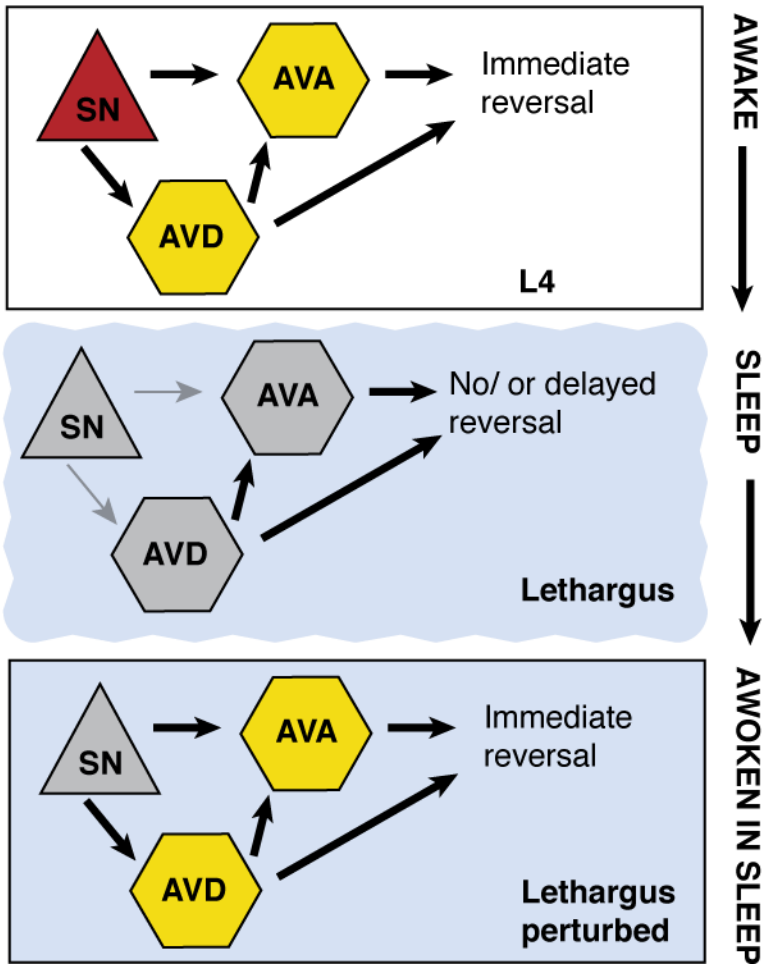

Figure 7. Waking sensitizes the interneurons for coordinated activity
Schematic model of activity during lethargus and waking during lethargus. Greyed neurons indicate decreased excitability: sensory neuron (SN) and the decreased excitability of or synaptic transmission of interneurons (AVD and AVA). Arrows mark synaptic connections between the neurons and the gray thin lines denote decrease in transmission across the sensory interneuron synapses in lethargus.

Supplementary Figure S1

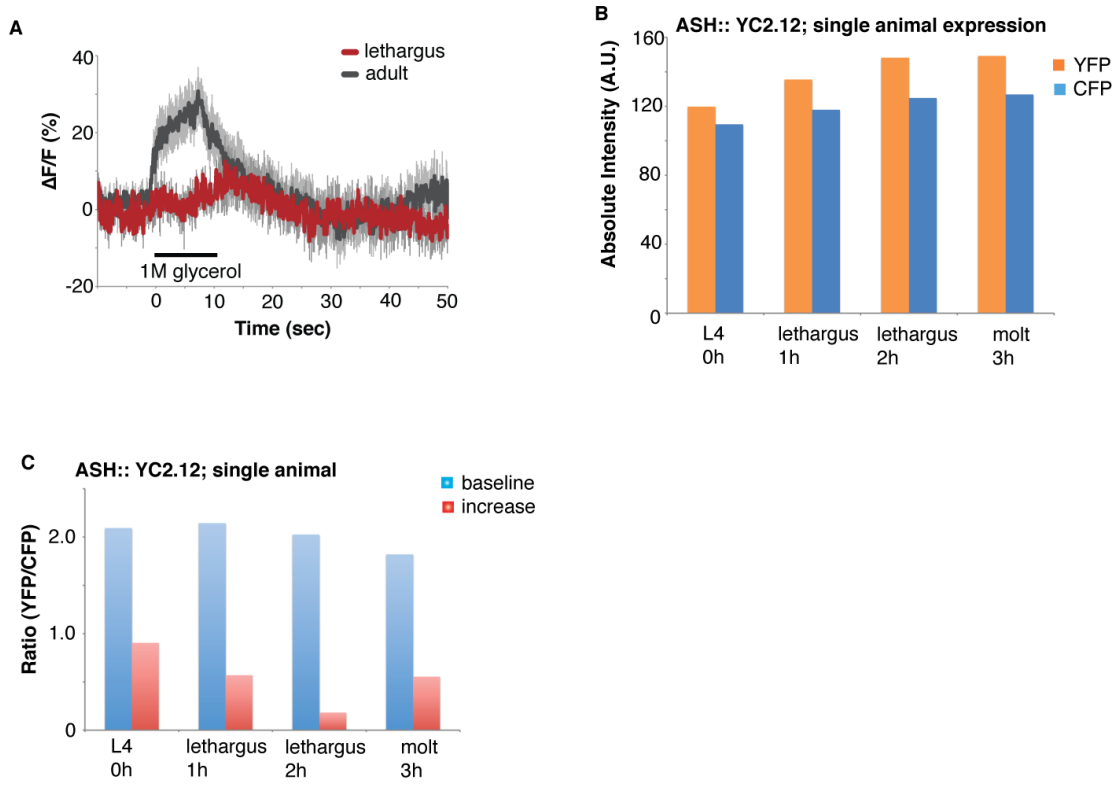

Supplementary Figure S1.
(A) Average Response 1M glycerol as measured by GCaMP3 in the ASH. Lethargus (n=25) and young adult (n=18). (B) Quantification of YFP and CFP expression in the ASH neuron of ASH::YC2.12 of one animal over time. **(C)** Quantification of baseline YFP/CFP ratio and amount of peak increase in ratio in response to 1mM Cu^{2+} in the ASH neuron of the same ASH::YC2.12 animal measure in B.

Supplementary Figure S2

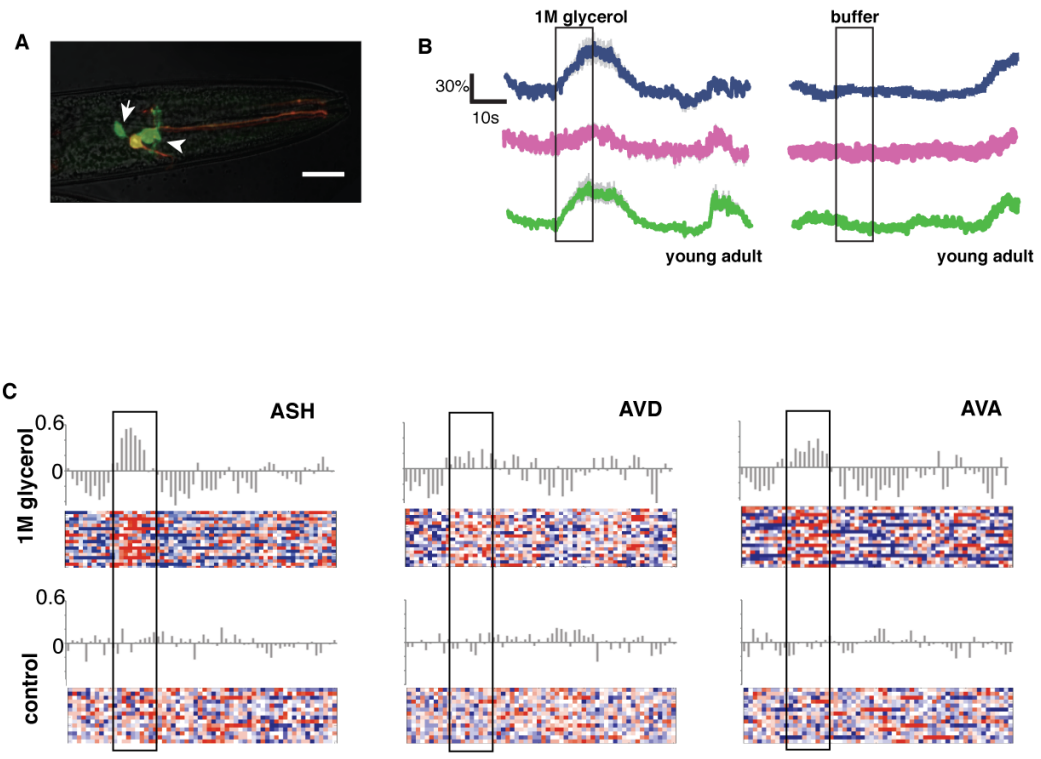

Supplementary Figure S2.
(A) Image of the neurons in which GCaMP3 was measured. ASH is marked by the presence of both GCaMP3 and mCherry, AVD is posterior (white arrow), and AVA is anterior (white arrowhead). (B) Representative traces of a glycerol trial in a single animal and representative traces of the control buffer trial. (C) Heat map of 60s trials denoting influx (red) and efflux (blue) in glycerol (n=18) and buffer (n=14). The proportion of influx or efflux were averaged across trials in 1s bins and are denoted by the gray bars above the heat maps.

Supplementary Figure S3

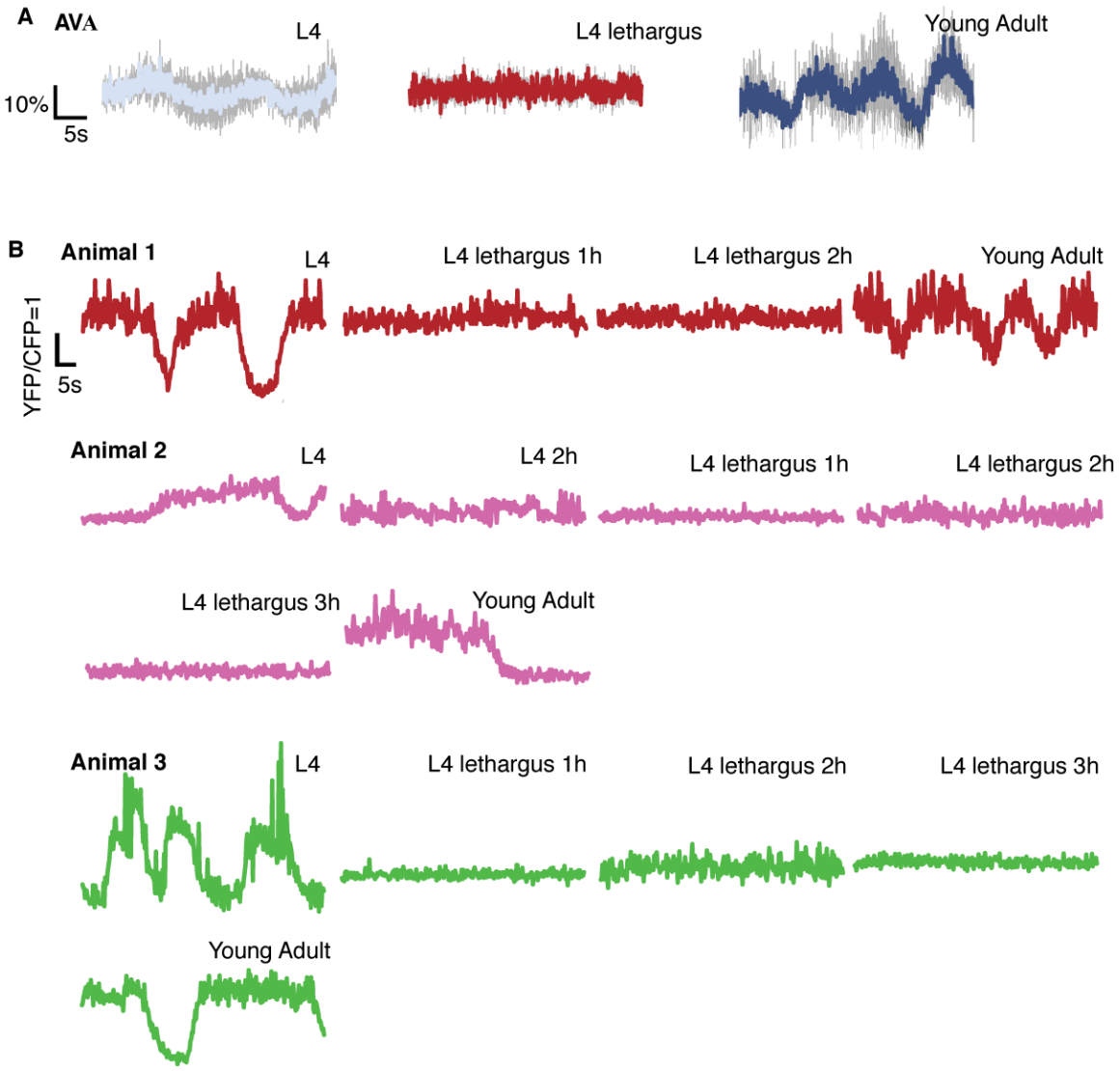

Supplementary Figure S3.
(A) AVA activity was measured by ratiometric FRET imaging. Representative individual traces are shown. The signal was calculated as the ratio of YFP to CFP emission at each time point. Intrinsic activity was measured during the 30s interval, and there are discernable calcium transients in the L4 worms. (B) AVA activity measured in individual worms over time. Intrinsic activity was measured during the 30s interval longitudinally as the worms went into and came out of lethargus.

Supplementary Figure S4

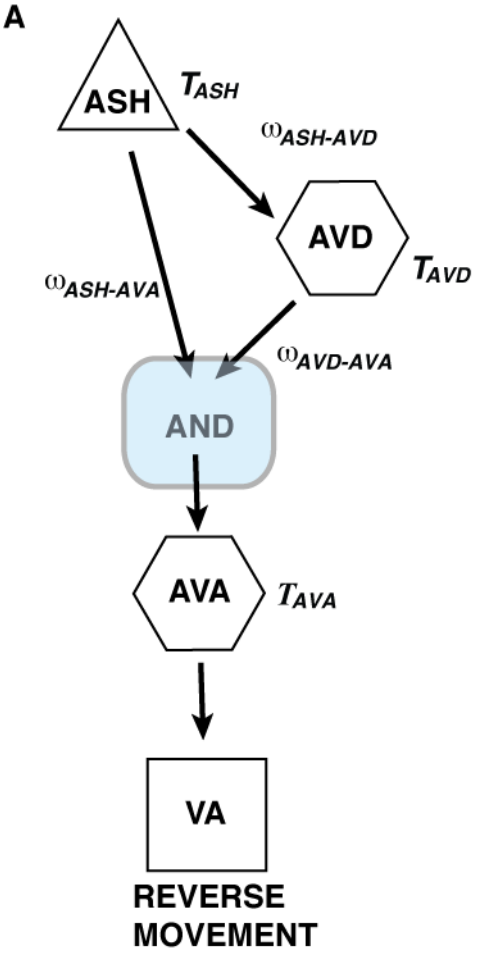

$dASH/dt = \beta(I > T_{ASH}) - \alpha\, ASH$

$dAVD/dt = \beta\,(ASH\,\omega_{ASH\text{-}AVD} > T_{AVD}) - \alpha\, AVD$

$dAVA/dt = \beta(ASH\;\omega_{ASH\text{-}AVA} + AVD\,\omega_{AVD\text{-}AVA} > T_{AVA}) - \alpha AVA$

$\alpha=1, \beta=1, \omega_i=1$

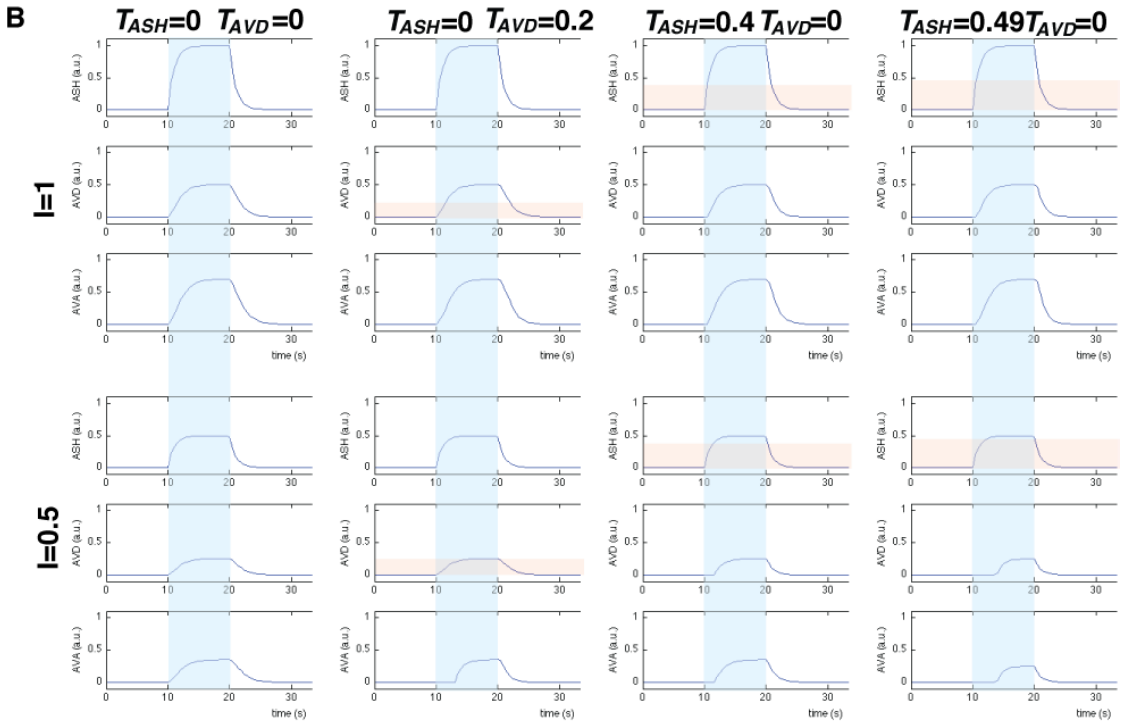

Supplementary Figure S4.
(A) Schematic of the feed forward loop. Equations from the model were adapted from those published.[29] (B) Simulation of dynamics built from the equations shown in (a). Threshold at ASH and AVD are adjusted to illustrated changes in dynamics at the downstream neurons. Input values were entered at I=1 and I=0.5. Previous published values for α=1 and β=1.[29]

Supplementary Figure S5

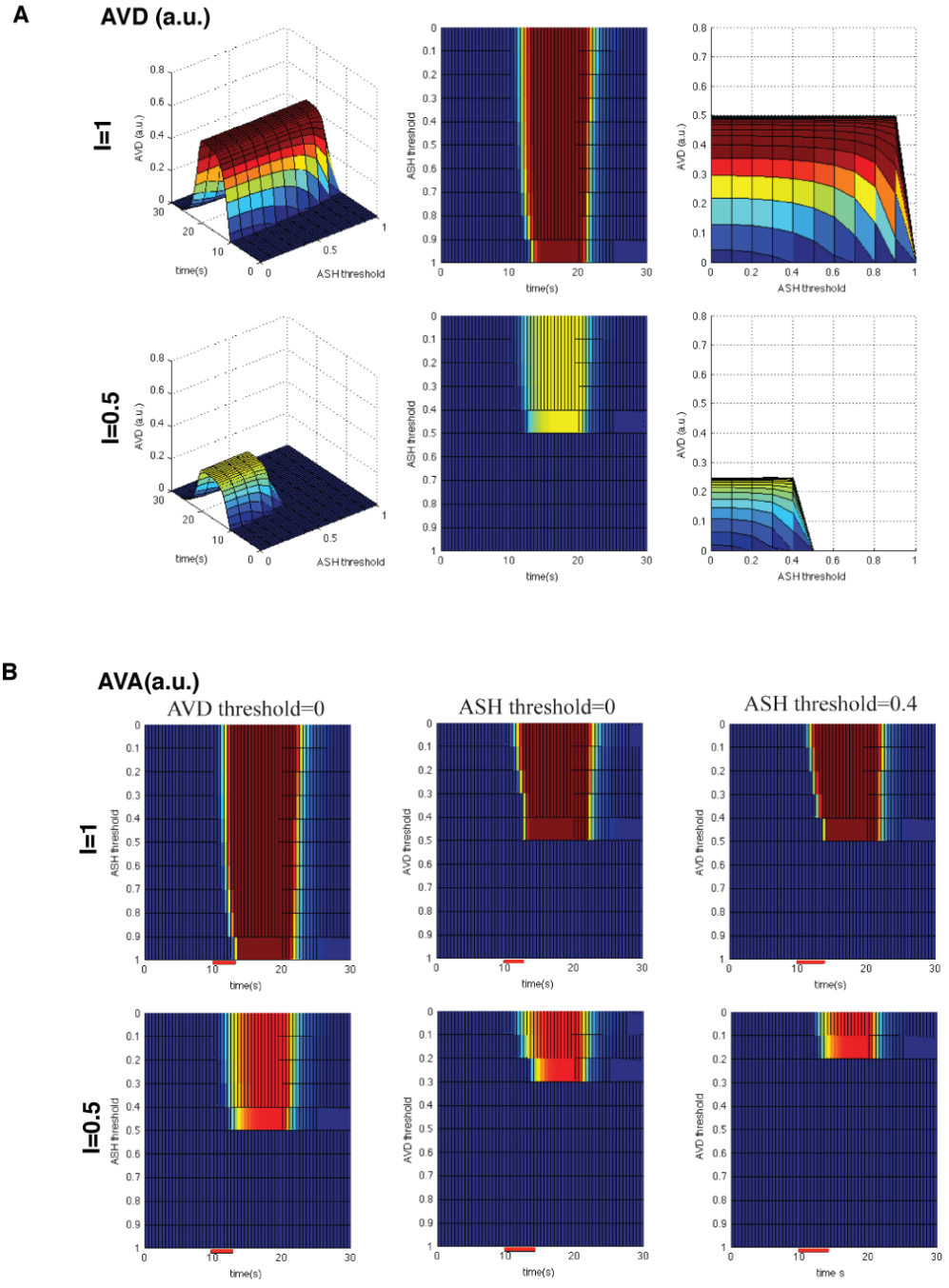

Supplementary Figure S5.
(A) Changes in timing and magnitude of AVD activity in response to input *I*=1 and *I*=0.5 at varying ASH thresholds. (B) Changes in timing and magnitude of AVA activity in response to input *I*=1 and *I*=0.5 at varying AVD and ASH thresholds.

Supplementary Figure S6

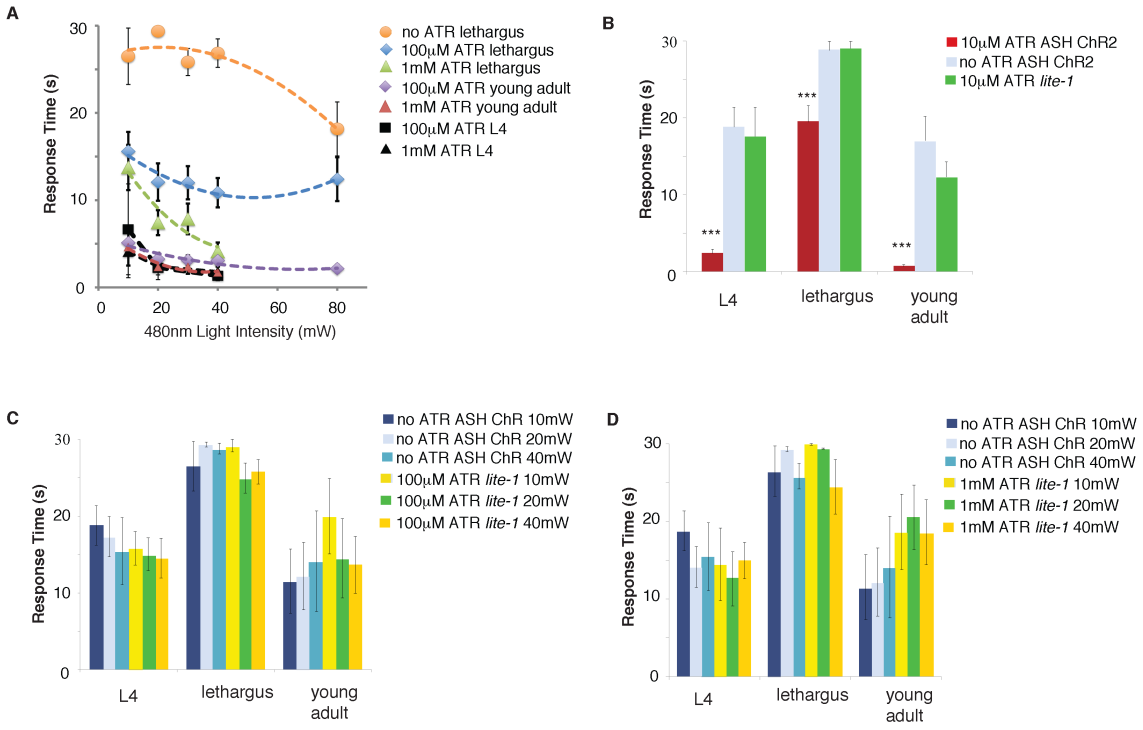

Supplementary Figure S6.
(A) Behavioral response to graded intensity of optical stimulation of ChR2 in L4, lethargus and young adult animals at 100µM and 1mM concentrations. (B) Reversal following light activation of the ASH neuron in animals grown on 10µM ATR as compared to no ATR control and *lite-1* grown on 10µM ATR. The mean ± s.e.m. values are shown: L4 (n=9), lethargus (n=12), adult (n=8), ***p=0.0001, ANOVA. (C) Control behavioral response to graded intensity of optical stimulation of ChR2 in L4, lethargus, and young adult animals at 100µM ATR concentration. The mean ± s.e.m. values are shown: L4 (n=19), lethargus(n=12), adult (n=8), NS, ANOVA. (D) Control behavioral response to graded intensity of optical stimulation of ChR2 in L4, lethargus, and young adult animals at 1mM ATR concentration. The mean ± s.e.m. values are shown: L4 (n=9), lethargus(n=7), adult (n=8), NS, ANOVA.

Supplementary Figure S7

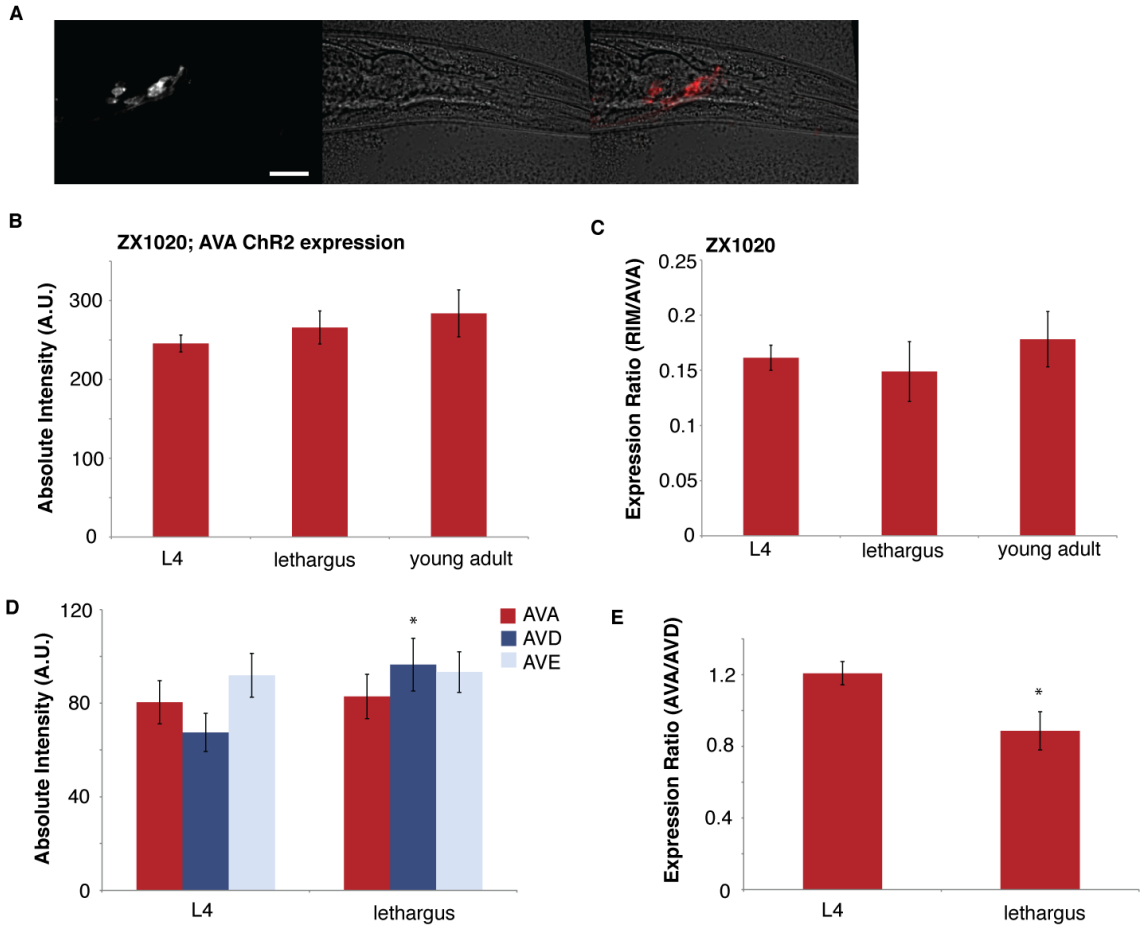

Supplementary Figure S7.
(A) Image of the *pnmr-1::ChR2::mcherry* expression (left=*mcherry*, middle= DIC, right= overlay). Expression is seen in 3 sets of neurons (AVA, AVD, and AVE). Scale bar is 20µm. **(B)** Quantification of ChR2::GFP expression in AVA of the ZX1020 animals during L4, lethargus, and young adult. The mean ± s.e.m. values are shown: L4 (n=10), lethargus (n=11), young adult (n=13), NS, ANOVA. **(C)** Quantification of the ratio of ChR2::GFP expression in the RIM and AVA of ZX1020 animals during L4, lethargus, and young adult. The mean ± s.e.m. values are shown: L4 (n=10), lethargus (n=6), young adult (n=12), NS, ANOVA. **(D)** Quantification of ChR2::mcherry expression in AVA, AVD, AVE of the *nmr-1* animals during L4, lethargus, and young adult. The mean ± s.e.m. values are shown: L4 (n=5), lethargus (n=5), *p<0.05, ANOVA. **(E)** Quantification of the ratio of ChR2::mcherry expression in the AVD and AVA of *nmr-1* animals during L4, lethargus, and young adult. The mean ± s.e.m. values are shown: L4 (n=5), lethargus (n=5), *p<0.05, Student's t-test of unequal variance.

Supplementary Figure 8

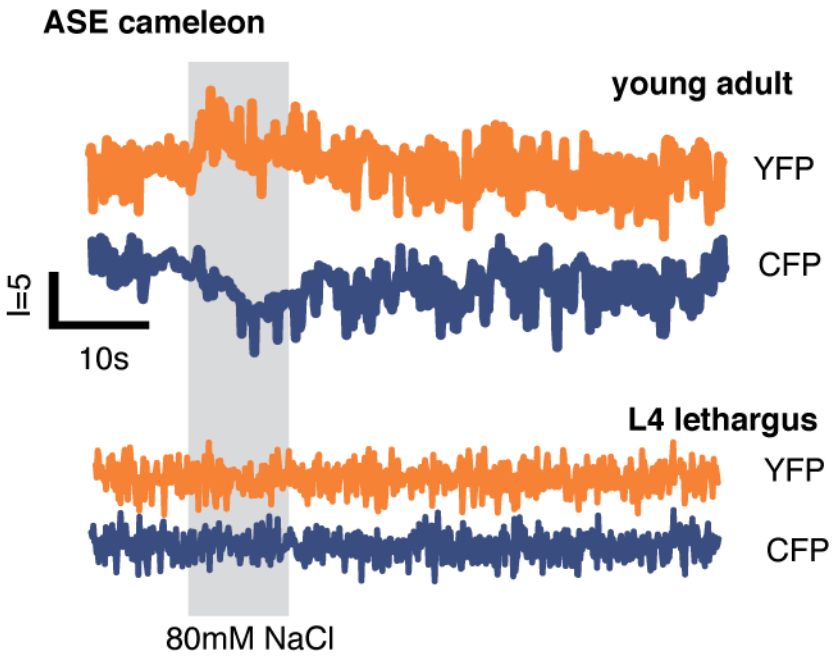

Supplementary Figure S8.
Representative traces of Cameleon measurements in the young adult and lethargus ASEL sensory neuron in response to 80mM NaCl.

METHODS

Strains. *Caenorhabditis elegans* strains were maintained under standard conditions at 20ºC (Brenner 1974). The following strains were used in this study:
ASH ChR2: AQ2235 *lite-1(ce314)*; *ljIs114[Pgpa-13::FLPase; Psra-6::FTF::ChR2::YFP]* [15],
AVA, RIM ChR2: **ZX1020** *lin-15(n765ts); lite-1(ce314); zxEx704[pflp18::loxP::LacZ::STOP::loxP:: ChR2::mCherry::SL2::GFP* (80 ng/µl); *pgpa-14::Cre* (80 ng/µl); *lin-15+]*[26],
Cholinergic motor neuron ChR2: **EG5096** [*Punc-17*:*ChR2*::*mCherry*] [27],
ASH ChR2 with ASH, AVD, and AVA GCaMP3: SRS85 *sraIs49 [nmr-1p::G-CaMP; unc-119(+)]; lite-1(ce314); sraEx80 [sra-6p::chop-2(H134R)::mCherry; osm-10p::G-CaMP; unc-122p::mCherry]* [14],
AVA cameleon: PS5955 (*Prig-3:: cameleon*),
ASH cameleon: *ljEx95[Psra-6::YC2.12]*[13] .

Molecular biology. The genetically encoded light-activated channelrhodopsin gene *ChR2* (a gift from the Deisseroth lab) was cloned into the pPD96.52 Fire vector (Addgene) to generate a *ChR2::YFP* fusion with the *unc-54 3'utr*. This construct was fused to a 5kb sequence from upstream of the *nmr-1* gene previously demonstrated to drive expression in AVA and AVD. Expression was confirmed in AVA, AVD, and AVD interneurons.[14]

Microfluidic device fabrication. We designed chips in AutoCAD (Autodesk) and sent the design to a mask-making service (Photosciences), which provided the chrome masks. We created the master molds by spin casting at 3,000 r.p.m and patterning a 19-µm-thick layer of SU-8 photoresist (MicroChem) on bare silicon wafers. We used previously published procedures to prepare the master molds for use with polydimethylsiloxane (PDMS) and perform the soft lithography to make the PDMS replicas. [38] The PDMS replicas were treated with air plasma (40W for 12s) to activate the PDMS surface and manually bond it to a coverslip. The PDMS devices were ethanol treated and flushed with FU-18 before use.

Calcium imaging. Calcium imaging was performed in a microfluidic device essentially as described.[17] The device was altered in only the part of the chip that constrains the worm to fit different developmental stages. Several versions were made in which the dimensions were scaled

to fit an animal 600µm in length and 30-60µm in diameter. The flow of stimuli and buffers in the device was controlled using an external valve system to regulate pressure at the various inlets, which modified the pattern of flow. External components were built according to published protocols to automate the valve system (Rafael Gómez-Sjöberg, Microfluidics Lab, Lawrence Berkeley National Laboratory), and valves were controlled using LabView software (National Instruments). Fluorescence time-lapse imaging (100-ms exposures, 5Hz) was performed on a Zeiss Axioscope inverted microscope with a 40x air objective and an Andor EMCCD camera. Animals were presented with alternating streams of S-basal complete buffer and stimulant (Cu2+ or glycerol) in S-complete buffer. All image analysis was done using a custom script written in Matlab: after background subtraction, total fluorescence intensity was measured from the individual regions of interest (ROIs) corresponding to the cell body. No adjustments were done for photobleaching as there was minimal evidence of such with the low intensity light exposure.

Analysis of Calcium Events. Exponential smoothing of the calcium imaging data was performed in Matlab (alpha value of 0.05) and instantaneous time derivatives were calculated for each time point. These values were plotted in a raster plot (Figures 2c, S4c) and were characterized as an influx (>0) or efflux (<0). These events were further binned into one-second bins to quantify the probability of these events during the duration of the imaging and response to buffer or glycerol. Cross correlation was performed on the data of corresponding ASH-AVD, ASH-AVA, and AVD-AVA traces. The value at lag time=0 or peak correlation was used to assess differences between different neuron sets and conditions.

Behavior. Unless otherwise stated, AQ2235 animals were grown in the dark with 10µM ATR and were illuminated with blue light (425–475 nm) from an LED device (Phillips LumiLEDS) at 12mW intensity at the level of the plate. EG5096 and ZX1020 animals were grown in the dark with 100µM ATR, picked onto a new ATR plate, allowed to rest for 10 minutes, and were illuminated with blue light (425–475 nm) from an LED device (Phillips LumiLEDS) at 12mW and 30mW intensity at the level of the plate. Animals were stimulated with an LED device when stationary or exhibiting forward locomotion, and imaged during the assay for behavioral analysis using a Leica stereomicroscope and a Unibrain camera using Unibrain software. Reversal was scored as posteriorwards movement that was greater than the length of the worm's head. Three trials were performed for each worm, and the interval between trials was 30 seconds.

Worms were perturbed for the waking assays by harsh touch with a worm pick immediately anterior to the middle of the worm (marked by the vulva), or by tail touch with an eyelash drawn across the tail of the worm. ChR2 assays were performed when the animals exhibited stationary behavior or forward locomotion (all stimulations were performed within 30 seconds of the perturbation).

Modeling. All simulations were performed using custom scripts in Matlab with parameters and equations previously published.[29] Individual variables (e.g. ASH activity), were generated by allowing the script to generate values at the various input values where other variables (ASH threshold, AVD threshold, AVA threshold) were fixed. The script ran variations of different combinations to generate the data plotted in the activity vs. time plots and the surface plots that are shown in Figures S2 and S3.

REFERENCES

[1] Allada, R. & Siegel, J. M. Unearthing the phylogenetic roots of sleep. *Curr. Biol.* **18**, R670-R679, doi:10.1016/j.cub.2008.06.033 (2008).

[2] Siegel, J. M. The REM sleep-memory consolidation hypothesis. *Science* **294**, 1058-1063, doi:10.1126/science.1063049 (2001).

[3] Van Buskirk, C. & Sternberg, P. W. Epidermal growth factor signaling induces behavioral quiescence in Caenorhabditis elegans. *Nat. Neurosci.* **10**, 1300-1307, doi:nn1981 [pii]10.1038/nn1981 (2007).

[4] Raizen, D. M. *et al.* Lethargus is a Caenorhabditis elegans sleep-like state. *Nature* **451**, 569-572, doi:nature06535 [pii]10.1038/nature06535 (2008).

[5] You, Y. J., Kim, J., Raizen, D. M. & Avery, L. Insulin, cGMP, and TGF-beta signals regulate food intake and quiescence in C. elegans: a model for satiety. *Cell Metab.* **7**, 249-257, doi:S1550-4131(08)00006-5 [pii]10.1016/j.cmet.2008.01.005 (2008).

[6] Monsalve, G. C., Van Buskirk, C. & Frand, A. R. LIN-42/PERIOD controls cyclical and developmental progression of C. elegans molts. *Curr. Biol.* **21**, 2033-2045, doi:10.1016/j.cub.2011.10.054 (2011).

[7] Zimmerman, J. E., Naidoo, N., Raizen, D. M. & Pack, A. I. Conservation of sleep: insights from non-mammalian model systems. *Trends Neurosci.* **31**, 371-376, doi:S0166-2236(08)00133-1 [pii]10.1016/j.tins.2008.05.001 (2008).

[8] Foltenyi, K., Greenspan, R. J. & Newport, J. W. Activation of EGFR and ERK by rhomboid signaling regulates the consolidation and maintenance of sleep in Drosophila. *Nat. Neurosci.* **10**, 1160-1167, doi:10.1038/nn1957 (2007).

[9] Ward, S., Thomson, N., White, J. G. & Brenner, S. Electron microscopical reconstruction of the anterior sensory anatomy of the nematode Caenorhabditis elegans.?2UU. *J. Comp. Neurol.* **160**, 313-337, doi:10.1002/cne.901600305 (1975).

[10] White, J. G., Southgate, E., Thomson, J. N. & Brenner, S. The structure of the nervous system of the nematode Caenorhabditis elegans. *Philosophical transactions of the Royal Society of London. Series B, Biological sciences* **314**, 1-340 (1986).

[11] Bargmann, C. I. Chemosensation in C. elegans. *WormBook : the online review of C. elegans biology*, 1-29, doi:10.1895/wormbook.1.123.1 (2006).

[12] Hilliard, M. A., Bargmann, C. I. & Bazzicalupo, P. C. elegans responds to chemical repellents by integrating sensory inputs from the head and the tail. *Curr. Biol.* **12**, 730-734 (2002).

[13] Hilliard, M. A. *et al.* In vivo imaging of C. elegans ASH neurons: cellular response and adaptation to chemical repellents. *EMBO J* **24**, 63-72, doi:10.1038/sj.emboj.7600493 (2005).

[14] Guo, Z. V., Hart, A. C. & Ramanathan, S. Optical interrogation of neural circuits in Caenorhabditis elegans. *Nat. Methods* **6**, 891-896, doi:10.1038/nmeth.1397 (2009).

[15] Ezcurra, M., Tanizawa, Y., Swoboda, P. & Schafer, W. R. Food sensitizes C. elegans avoidance behaviours through acute dopamine signalling. *EMBO J* **30**, 1110-1122, doi:10.1038/emboj.2011.22 (2011).

[16] Garrison, J. L. *et al.* Oxytocin/vasopressin-related peptides have an ancient role in reproductive behavior. *Science* **338**, 540-543, doi:338/6106/540 [pii]10.1126/science.1226201.

[17] Chronis, N., Zimmer, M. & Bargmann, C. I. Microfluidics for in vivo imaging of neuronal and behavioral activity in Caenorhabditis elegans. *Nat. Methods* **4**, 727-731, doi:nmeth1075 [pii]10.1038/nmeth1075 (2007).

[18] Yizhar, O., Fenno, L. E., Davidson, T. J., Mogri, M. & Deisseroth, K. Optogenetics in neural systems. *Neuron* **71**, 9-34, doi:10.1016/j.neuron.2011.06.004 (2011).

[19] Schwarz, J., Lewandrowski, I. & Bringmann, H. Reduced activity of a sensory neuron during a sleep-like state in Caenorhabditis elegans. *Curr. Biol.* **21**, R983-984, doi:10.1016/j.cub.2011.10.046 (2011).

[20] Ben Arous, J., Tanizawa, Y., Rabinowitch, I., Chatenay, D. & Schafer, W. R. Automated imaging of neuronal activity in freely behaving Caenorhabditis elegans. *J. Neurosci. Methods* **187**, 229-234, doi:10.1016/j.jneumeth.2010.01.011 (2010).

[21] Zhang, F. *et al.* Multimodal fast optical interrogation of neural circuitry. *Nature* **446**, 633-639, doi:nature05744 [pii]10.1038/nature05744 (2007).

[22] Narayan, A., Laurent, G. & Sternberg, P. W. Transfer characteristics of a thermosensory synapse in Caenorhabditis elegans. *Proc. Natl. Acad. Sci. U. S. A.* **108**, 9667-9672, doi:10.1073/pnas.1106617108 (2011).

[23] Lindsay, T. H., Thiele, T. R. & Lockery, S. R. Optogenetic analysis of synaptic transmission in the central nervous system of the nematode Caenorhabditis elegans. *Nature communications* **2**, 306, doi:10.1038/ncomms1304 (2011).

[24] Chalfie, M. *et al.* The neural circuit for touch sensitivity in Caenorhabditis elegans. *J. Neurosci.* **5**, 956-964 (1985).

[25] Piggott, B. J., Liu, J., Feng, Z., Wescott, S. A. & Xu, X. Z. The neural circuits and synaptic mechanisms underlying motor initiation in C. elegans. *Cell* **147**, 922-933, doi:10.1016/j.cell.2011.08.053 (2011).

[26] Schmitt, C., Schultheis, C., Husson, S. J., Liewald, J. F. & Gottschalk, A. Specific expression of channelrhodopsin-2 in single neurons of Caenorhabditis elegans. *PLoS One* **7**, e43164, doi:10.1371/journal.pone.0043164 (2012).

[27] Dabbish, N. S. & Raizen, D. M. GABAergic synaptic plasticity during a developmentally regulated sleep-like state in C. elegans. *J. Neurosci.* **31**, 15932-15943, doi:31/44/15932 [pii]10.1523/JNEUROSCI.0742-11.2011 (2011).

[28] Dabbish, N. S. & Raizen, D. M. GABAergic synaptic plasticity during a developmentally regulated sleep-like state in C. elegans. *J. Neurosci.* **31**, 15932-15943, doi:31/44/15932 [pii]10.1523/JNEUROSCI.0742-11.2011.

[29] Kashtan, N., Itzkovitz, S., Milo, R. & Alon, U. Topological generalizations of network motifs. *Physical review. E, Statistical, nonlinear, and soft matter physics* **70**, 031909 (2004).

[30] Chatzigeorgiou, M. & Schafer, W. R. Lateral facilitation between primary mechanosensory neurons controls nose touch perception in C. elegans. *Neuron* **70**, 299-309, doi:10.1016/j.neuron.2011.02.046 (2011).

[31] Li, W., Kang, L., Piggott, B. J., Feng, Z. & Xu, X. Z. The neural circuits and sensory channels mediating harsh touch sensation in Caenorhabditis elegans. *Nature communications* **2**, 315, doi:10.1038/ncomms1308 (2011).

[32] Schmitt, C., Schultheis, C., Husson, S. J., Liewald, J. F. & Gottschalk, A. Specific expression of channelrhodopsin-2 in single neurons of Caenorhabditis elegans. *PLoS One* **7**, e43164, doi:10.1371/journal.pone.0043164PONE-D-12-16560 [pii].

[33] Metherate, R. & Hsieh, C. Y. Synaptic mechanisms and cholinergic regulation in auditory cortex. *Prog. Brain Res.* **145**, 143-156 (2004).

[34] Metherate, R. Nicotinic acetylcholine receptors in sensory cortex. *Learn Mem.* **11**, 50-59, doi:10.1101/lm.69904 (2004).

[35] Letzkus, J. J. *et al.* A disinhibitory microcircuit for associative fear learning in the auditory cortex. *Nature* **480**, 331-335, doi:10.1038/nature10674 (2011).

[36] Magnin, M. *et al.* Thalamic deactivation at sleep onset precedes that of the cerebral cortex in humans. *Proc. Natl. Acad. Sci. U. S. A.* **107**, 3829-3833, doi:10.1073/pnas.0909710107 (2010).

[37] Jones, E. G. Synchrony in the interconnected circuitry of the thalamus and cerebral cortex. *Annals of the New York Academy of Sciences* **1157**, 10-23, doi:10.1111/j.1749-6632.2009.04534.x (2009).

[38] Park, J. W., Vahidi, B., Taylor, A. M., Rhee, S. W. & Jeon, N. L. Microfluidic culture platform for neuroscience research. *Nat. Protoc.* **1**, 2128-2136, doi:nprot.2006.316 [pii]10.1038/nprot.2006.316 (2006).